HAL
open science

Characterization and role of intra-hepatic regulatory T cells in chronic hepatitis C pathogenesis.

Nathalie Sturm, Marie-Ange Thélu, Xavier Camous, Guéorgui Dimitrov, Muhammad Ramzan, Tania Dufeu-Duchesne, Paula Bonorino, Christiane Guillermet, Elisabeth Brambilla, Philippe Arvers, et al.

To cite this version:

Nathalie Sturm, Marie-Ange Thélu, Xavier Camous, Guéorgui Dimitrov, Muhammad Ramzan, et al.. Characterization and role of intra-hepatic regulatory T cells in chronic hepatitis C pathogenesis.. Journal of Hepatology, 2010, 53 (1), pp.25-35. 10.1016/j.jhep.2010.02.024 . inserm-00509310

HAL Id: inserm-00509310

https://inserm.hal.science/inserm-00509310v1

Submitted on 11 Aug 2010

HAL is a multi-disciplinary open access archive for the deposit and dissemination of scientific research documents, whether they are published or not. The documents may come from teaching and research institutions in France or abroad, or from public or private research centers.

L'archive ouverte pluridisciplinaire **HAL**, est destinée au dépôt et à la diffusion de documents scientifiques de niveau recherche, publiés ou non, émanant des établissements d'enseignement et de recherche français ou étrangers, des laboratoires publics ou privés.

Characterization and Role of Intra-Hepatic Regulatory T Cells in Chronic Hepatitis C Pathogenesis

Nathalie Sturm[1,2,3*], Marie-Ange Thélu[1,2*], Xavier Camous[1,2], Guéorgui Dimitrov[1,2], Muhammad Ramzan[1,2], Tania Dufeu-Duchesne[1,2], Paula Bonorino[1,2], Christiane Guillermet[2,3], Elisabeth Brambilla[1,2,3], Philippe Arvers[4], Martine Pernollet[1,2], Vincent Leroy[1,2] , Jean-Pierre Zarski[1,2], Patrice N.Marche[1,2**] and Evelyne Jouvin-Marche[1,2**].

1 INSERM, Unité 823, Grenoble, France
2 Université Joseph Fourier-Grenoble I, Institut Albert Bonniot, UMR-S823, Grenoble, France.
3 Département d'Anatomie et de Cytologie Pathologiques, Pôle de Biologie, CHU A Michallon, 38043, Grenoble, France
4 Centre de recherche de Service de Santé des Armées, La Tronche, France
* NS and MAT have contributed equally to this work
**PNM and EJM have contributed equally to this work

Correspondance
Institut Albert Bonniot, Centre de Recherche INSERM-UJF U823
Equipe Immunologie Analytique des Pathologies Chroniques
UJF Site Santé BP 170 Grenoble 38042 Cedex 9 France
Mail: Marie-Ange.Thelu@ujf-grenoble.fr; patrice.marche@ujf-grenoble.fr
Phone: +33 (0) 476 54 94 95 **Fax:** +33 (0) 476 54 94 54

Key words: Hepatitis C Virus (HCV), Regulatory T cells, FoxP3, Immunohistochemistry, T lymphocytes, Liver.

Abstract

Background/aims: In chronic hepatitis C (CHC), HCV-specific T-cell responses are often dysfunctionnal. *In vitro* data point out that regulatory T cells (Treg) are able to suppress HCV-specific lymphocyte proliferation and cytokine secretion but their implication in this pathology is still debated.
Methods: Three complementary approaches were performed to investigate phenotype, frequency or localization of intra-hepatic Treg in treatment naïve CHC patients. Double immunohistochemical analysis was performed in 20 formalin-fixed biopsies with CD8/FoxP3 and CD4/FoxP3 antibodies. Cellular markers and cytokines were investigated by quantitative RT-PCR in 27 additional frozen biopsies. Eight other fresh liver biopsies were selected for complementary analysis of immunophenotyping and frequency of intra-hepatic Treg.
Results: Immunohistochemical analyses showed the presence of intra-hepatic $CD4^+FoxP3^+$T cells while $CD8^+FoxP3^+$T cells were very scarce. $CD4^+FoxP3^+$T cells were located in necro-inflammatory areas in contact with $CD8^+$T cells, suggesting that Treg-mediated inhibition of $CD8^+$T cell proliferation may occur by cell-cell contact. RT-PCR analyses showed strong correlations between CD8, FoxP3 and IL-10 with emergence of four distinct gene clusters, CD8-FoxP3, CD8-IL-10, TGF-β–IL-10 and TNF-α-TGF-β. No correlation was found between serum viral load and any immune markers. Interestingly, the $FoxP3^+/CD8^+$ cells ratio significantly decreased in severe fibrosis (F>3) due to dramatic decline of FoxP3 cells.
Conclusions: This study provides new insights into the histological localization of Treg within HCV-infected liver, with a special accumulation of $CD4^+FoxP3^+$Treg cells in necro-inflammatory areas, in contact with $CD8^+$T cells. Our results suggest a link between Treg, CD8 and IL-10 which altogether could balance immune responses against the virus to avoid immunopathogenesis.

Introduction

In chronic hepatitis C (CHC), blood $CD4^+$T and $CD8^+$T cell responses have limited impact on disease course [1-3] but intra-hepatic T lymphocytes seem to control disease pathogenesis [4-6]. Therefore, regulation of intra-hepatic T cell responses in Hepatitis C Virus (HCV) patients may have important implication not only in determining spontaneous clearance but also in disease progression during chronic infection [7-9].

It is well known that $CD4^+CD25^+$T cells are activated by microbial infections, leading to an overall increase of anti-inflammatory cytokines. The increase in these cytokines induces the suppressive functions of $CD4^+CD25^+$ natural regulatory T cells (Treg) [10-14] and could promote their local survival or retention [15]. Finally, infections disturb balance between natural Treg and effector lymphocytes, thereby alter immune response and may contribute to disease progression.

It has been shown that HCV patients have a higher number of Treg in peripheral blood than healthy patients [16-18]. When the natural Treg pressure is removed, the effector function of $CD8^+$T cells is restored and viral load is considerably reduced [19]. Depletion of $CD4^+CD25^+$T cells enhances antigen-specific $CD4^+$T and $CD8^+$T proliferation and response [11, 18, 20]. All these data have demonstrated that Treg play a key role in HCV disease.

Nowadays, Treg defined as $CD4^+CD25^+$ are also characterized by expression of the transcriptional factor Forkhead box Protein 3 (FoxP3) [21, 22]. Comparisons of $CD4^+CD25^+FoxP3^+$ Treg between infected and uninfected-HCV patients show that they are phenotypically, functionally and genetically indistinguishable [23, 24]. Among HCV-infected patients, HCV-specific $FoxP3^+$Treg are detected in the blood and have the capacity to suppress HCV-specific T cells [23].

Previous *in vitro* data point out the presence of Treg expressing CD8 with regulatory ability [25-27]. Nevertheless, frequency and biological role of human $CD8^+FoxP3^+$T cells is less understood than their $CD4^+CD25^+FoxP3^+$T counterparts**.** Stimulation of peripheral blood mononuclear cells (PBMC) with HCV peptides reveals the presence of both virus-specific $CD8^+FoxP3^-$ and $CD8^+FoxP3^+$T cells. $CD8^+FoxP3^+$T cells have proliferative capacity and display a cell-cell contact-dependent suppressive activity [28].

In HCV infection, most of studies are focused on peripheral Treg which probably do not reflect the precise composition and functions of these cells in the liver. In order to examine the physiopathological implication of intra-hepatic Treg during CHC, we evaluated their *ex vivo* phenotype, frequency and histological localization by immunohistochemistry and flow cytometry, and quantified intra-hepatic cytokines by RT-PCR, in relation to virological and histological parameters.

2. Patients and Methods

2.1. Patients and Material

Liver biopsies from chronically HCV-infected patients seen in Grenoble Hospital were selected from 2003 to 2005. Each patient had serological markers of HCV infection and presence of HCV RNA in serum. They were naïve of current or past immunomodulatory or antiviral treatment and had a frozen liver sample available. Fresh liver biopsies obtained by using 1.5 mm diameter disposable needle biopsy were divided into one part for histopathological examination (activity grading and fibrosis staging according to Metavir scoring system assessed by an experienced liver pathologist) and another part for immunological analyses. Blood samples from patients were collected at time of biopsy in heparinized vacutainer tubes. In practice, 47 frozen liver samples were retrospectively available for quantitative RT-PCR analyses and immunohistochemical analyses were performed in a sub-group of 20 formalin-fixed biopsies. Eight additional liver biopsies were prospectively included for exclusive flow cytometry analysis which needed fresh tissue samples and larger amount of cells for phenotyping (Table 1). Criteria for exclusion were age under 18 years, presence of AgHBs or anti-HIV antibodies, other causes of chronic liver disease, alcohol consumption higher than 30 g/day. The study was in agreement with the recommendations of the local ethics committee and all patients gave written informed consent.

2.2. Double immunohistochemical analysis

Double immunohistochemical labeling was performed manually (Sequenza station) on 20 formalin-fixed, paraffin-embedded liver biopsies. Two methods of immunodetection were applied: streptavidin-biotin-peroxydase (SBP) method with diaminobenzidine (DAB) as chromogen and streptavidin-biotin-alkaline phosphatase (SBAP) method with fast blue (FB) as chromogen.

For CD8/FoxP3 double staining, primary mouse anti-CD8 antibody (CD8, clone C8/144B, 1/100, *Dako, Carpinteria, USA*) and secondary biotinylated goat anti-mouse antibody (1/500, *Jackson ImmunoResearch, West Grove, USA*) were used, followed by detection with SBAP complex (1/50, *Dako*) and FB chromogen staining. For FoxP3 staining, primary mouse antibody (FoxP3, 1/20, *Abcam, Cambridge, UK*) and secondary biotinylated goat anti-mouse antibody (1/500, *Jackson ImmunoResearch*) were used, and detection was performed with SBP complex (1/200, *Dako*) and DAB chromogen staining.

For CD4/FoxP3 double staining, primary mouse antibody (CD4, clone 4B12, 1/75, *Novocastra, Newcastle, UK*), endogenous peroxydase inhibition, incubation with secondary biotinylated goat anti-mouse antibody, detection with SBP complex and DAB chromogen staining were performed. The second immunostaining with FoxP3 was performed as above with SBAP method and FB staining. Staining with an unrelated primary antibody (mouse IgG, 2 µg/ml, *Jackson ImmunoResearch*) provided a negative control for each reaction.

Positive cells were counted on a computer screen in consecutive fields along the whole section of the biopsy as described previously [29], with the help of automatic software LUCIA (*Laboratory Universal Computer Image Analysis, version 5.0, Laboratory Imaging, Prague, Czech Republic*). Cell counts were performed by a single liver pathologist (NS) on serial sections obtained from paraffin blocks. Recorded parameters included total number of $CD8^+$, $CD4^+$ and $FoxP3^+$ cells, and distribution of $FoxP3^+$ cells in fibrotic tissue (fibrous septa and portal tracts), in parenchymatous areas (lobules or nodules) and in foci of piecemeal or lobular necrosis. Results were expressed as number of cells per field, at magnification X20 (1.002 mm^2).

Table 1. Demographic, biochemical and histological characteristics in chronic hepatitis C (CHC) patients

	CHC patients groups *		
	studied by RT/PCR *(n=47)*	**studied by histochemistry** *(n=20)*	**studied by flow cytometry** *(n=8)*
Male, n (%)	32 (68%)	15 (75%)	4 (50%)
Age (y)*	43 (24-75)	44 (24-75)	53 (32-75)
Plasma Viral Load (logIU/mL)	6.1± 6.2	6.1± 6.1	6.0± 0,6
Serum ALT (IU/mL)	130.1 ± 98.8	172.6 ± 105.5	118.6 ± 95,8
Histology* **			
Metavir Activity, n (%)			
0	0	0	-
1	20 (43%)	4 (20%)	2 (25%)
2	18 (38%)	9 (45%)	5 (63%)
3	9 (19%)	7 (35%)	1 (13%)
Metavir Fibrosis, n (%)			
0	7 (15%)	1 (5%)	-
1	12 (26%)	3 (15%)	3 (38%)
2	14 (30%)	7 (35%)	4 (50%)
3	10 (21%)	6 (30%)	-
4	4 (8%)	3 (15%)	1 (13%)

* Mann et Whitney statistical analysis did not reveal any difference in term of demographic, biochemical and histological characteristics between the 3 groups of patients.
** Median (Range)
*** Number of cases / total (%)
ALT: Alanine Aminotransferase

2.3. RT-PCR analysis

Total RNA (5-10 mg) was extracted from 47 frozen liver biopsies, by homogenization of tissues in silica balls using MagnaLyser System (*Roche Diagnostics, Meylan, France*). The mixture was filtered on a silica column and "digested" by DNase I. Single-stranded cDNA was synthesized from 5-10 µg of total RNA by using the Superscript II Reverse Transcriptase (*Gibco BRL, Life Technologies, Bethesda, USA*). Primer pairs and probes for quantification of CD4, CD8-β, FoxP3, IL-10, IFN-γ, TGF-β, and TNF-α genes (Table 2) were designed with ProbeFinder Software for Human (version 2.35, *Roche Diagnostics*). Quantification of transcripts was performed with the LightCycler® 480 Real-Time PCR System *(Roche Diagnostics*) and target sequences were detected with UPL (Universal ProbeLibrary, *Roche Diagnostics*). Data were analyzed with the LightCycler® 480 Software. The detection format was set to "Mono Colour Hydrolysis Probe" and the Second Derivative Maximum Method was used for absolute quantification. The housekeeping gene used for normalization of the values was the Hypoxanthine Phosphoribosyl Transferase gene (HPRT).

2.4. Immunostaining and flow cytometry analysis

Immunophenotyping was performed on 8 paired PBMC and liver samples with mouse monoclonal anti-FoxP3-PE (*Human/Non Human Primate Regulatory T Cells Staining Kit -BD Biosciences, Pont de Claix, France*), anti-human CD4-APC, anti-human CD8-FITC and anti-human CD25-PC7 (*Beckman Coulter, Villepinte, France*)

antibodies**.** PBMC were isolated by density centrifugation over Ficoll gradients. Fresh tissues were washed and disrupted mechanically. Immunostaining and flow cytometry analyses were done as previously described [30-32]. Briefly, we selected total viable lymphocytes (1) by excluding dead cells after propidium iodide staining and (2) by gating PBMC and intra-hepatic cells on the basis of the forward and side scatting, after checking their anti-human CD45 expression (*Beckman Coulter, Villepinte, France*). Total lymphocytes were then gated on basis of their CD4 or CD8 expression and each sub-population was gated on CD25 and FoxP3 expression.

2.5. Statistical methods

Statistical analysis was performed using SPSS 15.0 software (*SPSS Inc., Chicago, IL, USA*). Quantitative variables were compared with non-parametric Wilcoxon test and Mann-Whitney U-test. The 2-tailed Spearman's correlation coefficient was used for comparisons within group. Principal Component Analysis (PCA) and linear univariate and multivariate regression analyses were also performed. P values less than 0.05 were considered significant.

Table 2. Primers and Universal Probe Library (UPL) sequences used in the LightCycler® 480 Real-Time PCR System
F, Forward primer – R, Reverse primer

Genes		Primer Sequences	Product Length (nt)	UPL Sequences
CD4	F	agcgaaaacaggaaagttgc	**72**	**tggtgatg**
	R	aaatttttctggagctgagtgg		
CD8-β	F	caggccagagacccagaa	**84**	**gcctgctg**
	R	gaaaccagcagaaccaggac		
FoxP3	F	acctacgccacgctcatc	**65**	**gctccaga**
	R	tcattgagtgtccgctgct		
IL-10	F	tgggggagaacctgaagac	**62**	**ggctgagg**
	R	acagggaagaaatcgatgaca		
IFN-γ	F	ggcattttgaagaattggaaag	**112**	**cagagcca**
	R	tttggatgctctggtcatctt		
TGF-β	F	gcagcacgtggagctgta	**64**	**ttcctggc**
	R	cagccggttgctgaggta		
TNF-α	F	cagcctcttctccttcctgat	**123**	**cttctgcc**
	R	gccagagggctgattagaga		
HPRT	F	gaccagtcaacaggggacat	**95**	**tggtggag**
	R	gtgtcaattatatcttccacaatcaa g		

3. Results

3.1. Immunohistochemical analysis of intra-hepatic $CD4^+FoxP3^+$ and $CD8^+FoxP3^+$ cells

Analysis was performed in a sub-group of 20 patients who had similar characteristics than those of the whole population (**Table 1**). This procedure was adopted to visualize CD4, CD8 and FoxP3 single positive cells and CD4FoxP3 or CD8FoxP3 double positive cells (**Fig.1).** $CD4^+FoxP3^+$ co-stained cells were identified by a blue nuclear staining with anti-FoxP3 antibody, circled by a brown cytoplasmic membrane staining with anti-CD4 antibody. $CD8^+FoxP3^+$ co-stained cells were characterized by brown nuclear staining with anti-FoxP3 antibody, circled by blue cytoplasmic membrane staining with anti-CD8 antibody. More than 99.5% of $FoxP3^+$ cells were $CD4^+$ cells (**Fig.1A,B**). Nevertheless, among slides from 20 patients, we only detected two persuasive $CD8^+FoxP3^+$ cells (**Fig.1G,H**). This suggests that $CD8^+FoxP3^+$ cells are very scare in the liver and that the majority of $FoxP3^+$ cells co-express CD4. A considerable amount of $FoxP3^+$ cells were observed in portal tracts and fibrous septa **(Fig.1C),** particularly when lymphoid aggregates were present (**Fig.1D).** They were also observed in parenchymatous areas where they preferentially localized in necrotic areas in close contact with $CD8^+$T lymphocytes **(Fig.1E,F),** suggesting contact-dependent inhibition of the effector functions of $CD8^+$T cells by $FoxP3^+$ cells.

3.2. Histological relationship between intra-hepatic $FoxP3^+$ cells and $CD4^+$ or $CD8^+$ cells

Correlations between frequency and localization of $FoxP3^+$ and $CD4^+$ or $CD8^+$ lymphocytes were studied. Cells were counted on an average of 50 fields (20 to 105) per liver biopsy. A significant correlation was found between the total number of $FoxP3^+$ cells and the total number of $CD4^+$ cells (**Fig.2A**-r=0.508-p=0.022) or the total number of $CD8^+$ cells (**Fig.2B-**r=0.538-p=0.014). By multivariate linear regression analysis, only the correlation between total $CD8^+$ and $FoxP3^+$ cells remained significant (r=0.466-p=0.039). Correlations were also observed between the total number of $FoxP3^+$ cells and the number of $CD8^+$ cells in fibrotic and parenchymatous areas (r= 0.505-p=0.023 and r= 0.555-p=0.011 respectively, **Fig.2C,D).** Moreover, the total number of $FoxP3^+$ cells correlated with the number of $FoxP3^+$ cells in the fibrotic tissue (r=0.923-p<0.001), the parenchymatous areas (r=0.777-p<0.001) and the necro-inflammatory lesions (r=0.833-p<0.001). Interestingly, a strong correlation was observed between $CD8^+$ lymphocytes and $FoxP3^+$ cells in parenchymatous areas (r=0.511-p=0.021-**Fig.2E)**, especially inside the necro-inflammatory lesions (r=0.630-p=0.003-**Fig.2F),** suggesting that $FoxP3^+$ cells are mostly associated to $CD8^+$ cells. Corroborating this point, 22% of $FoxP3^+$ cells were present in the necro-inflammatory foci in contact with $CD8^+$ cells or apoptotic bodies.

3.3. Quantitative RT-PCR analysis of intra-hepatic CD4, CD8, FoxP3 and IL-10

To extend our analysis, RT-PCR was performed on 47 liver biopsy samples for the quantification of CD4, CD8, FoxP3, IL-10, TGF-β, IFN-γ and TNF-α transcripts. Results were expressed as a ratio between the number of amplicons from the target gene and from HPRT gene. PCA determined the presence of gene clusters (**Fig.3**). The most relevant correlations were observed between CD8 and FoxP3 (r=0.564-p=0.001-**Fig.3A),** CD8 and IL-10 (r=0.405-p=0.022-**Fig.3B),** TNF-α and TGF-β (r=0.652-p=0.005-**Fig.3C)** and TGF-β and IL-10 (r=0.688-p<0.001-**Fig.3D)**. Moreover, pro-inflammatory cytokines TNF-α and IFN-γ were also closely correlated to each other (r=0.496-p=0.004). Then, univariate and multivariate regression analyses were conducted for the correlated genes, with CD8 as the dependent variable and IL10, FoxP3, IFN-γ and TNF-α as

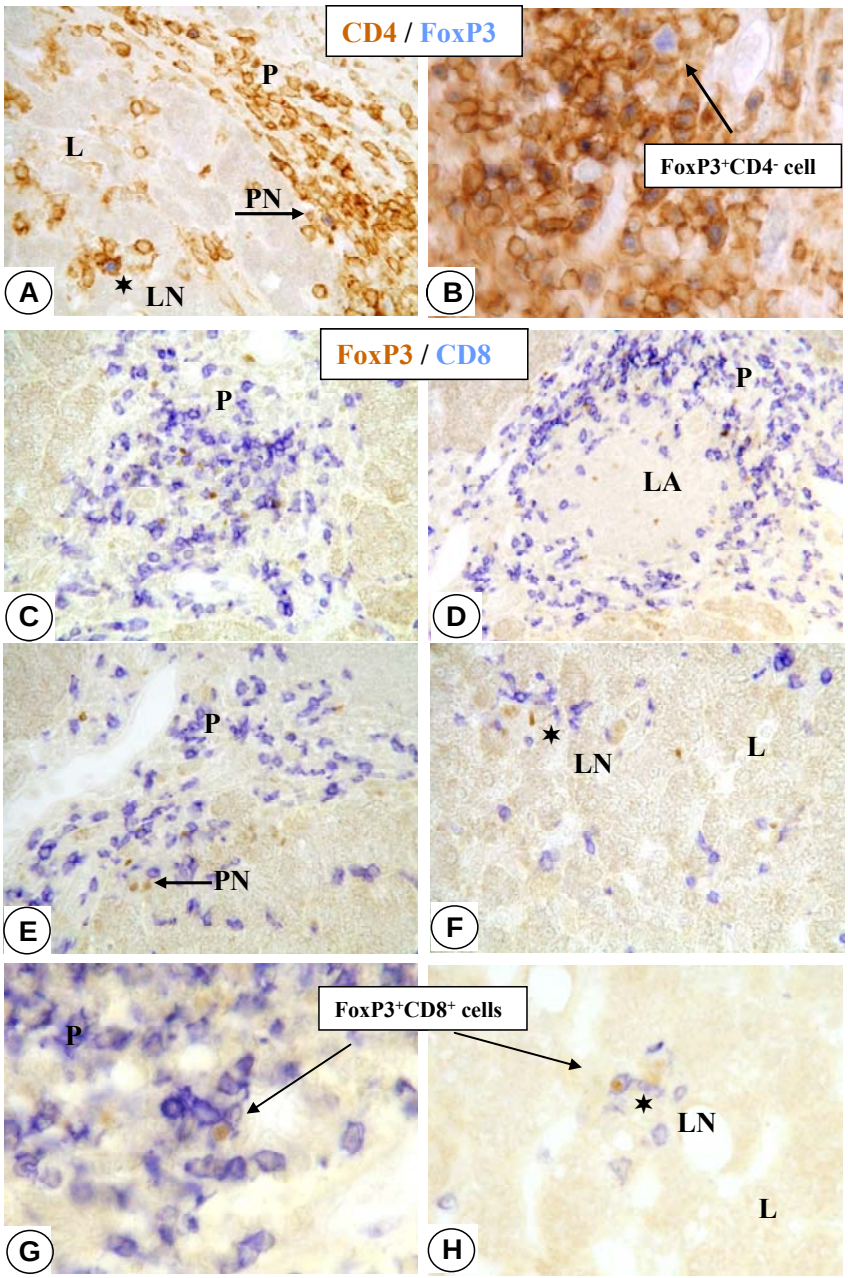

Fig.1. CD4/FoxP3 or CD8/FoxP3 double immunohistochemical labeling.
(A) Double CD4/FoxP3 immunohistochemical labeling showing $CD4^{+}FoxP3^{+}$ cells characterized by a blue nuclear FoxP3 staining and a brown cytoplasmic CD4 staining, in contact with foci of parcellar necrosis (PN, arrow) and lobular necrosis (LN, asterisk) in peri-portal (P) and lobular (L) areas (magnification x20)**.** **(B)** High magnification (x40) of CD4/FoxP3 immunolabeling in a portal tract showing that all FoxP3 cells were CD4 positive lymphocytes, except one blue FoxP3 cell without cytoplasmic CD4 staining (arrow). **(C)** Double CD8/FoxP3 immunohistochemical labeling showing numerous separate brown FoxP3 cells and blue CD8 lymphocytes, in a fibrous portal tract (magnification x20). **(D)** FoxP3 cells were particularly numerous in fibrous portal areas when nodular lymphoid aggregates **(LA)** were present (magnification x10). **(E)** Brown FoxP3 cells in contact with parcellar necro-inflammatory lesions (PN, arrow) in peri-portal areas (magnification x20). **(F)** Brown FoxP3 cells in contact with lobular necro-inflammatory lesions (LN, asterisk) in lobular areas (magnification x20). **(G,H)** High magnifications (x40) showing two putative double labeled CD8+FoxP3+ lymphocytes in a fibrous portal area **(G)** and in contact with lobular necrosis (LN, asterisk) in a lobule (**H**).

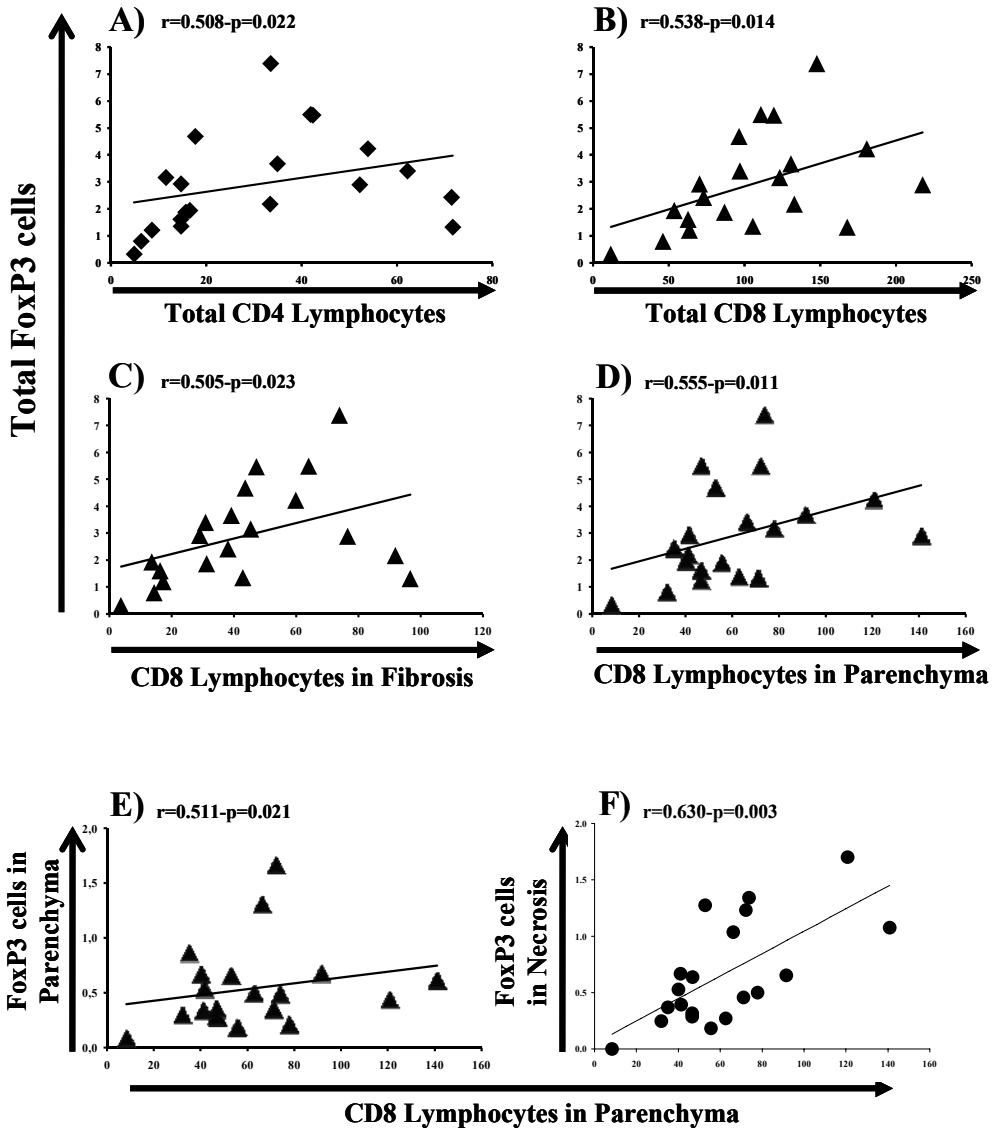

Fig.2. Relationship between intra-hepatic number of FoxP3 cells and CD4 or CD8 lymphocytes in different histological areas.
(A-D) Total number of FoxP3 cells was significantly correlated in chronic HCV-infected liver with total CD4 lymphocytes (**A**) and with total CD8 lymphocytes **(B)**, CD8 in fibrous septa **(C)** and CD8 in parenchyma **(D). (E,F)** In parenchymatous areas, FoxP3 cells and CD8 lymphocytes were statistically correlated **(E),** especially within necro-inflammatory areas (**F**).

independent variables. A regression model was deduced [CD8 = 0.88.IL-10–0.01.FoxP3+0.04.IFNγ (R^2=0.810-p<10^{-6})] and suggested that (i) when IL-10 expression increased by 1 unit, CD8 expression increased by 0.88 units, keeping the expression of FoxP3 and IFN-γ as constant (ii) when FoxP3 expression increased by 1 unit, CD8 expression decreased by 0.01 units, keeping the expression of IL-10 and IFN-γ as constant. Therefore, CD8, FoxP3 and IL-10 were linked together in the correlation circle of the PCA (**Fig.3E,F**)

3.4. Flow cytometry detection and quantification of intra-hepatic $CD4^+CD25^+FoxP3^+$ and $CD8^+CD25^+FoxP3^+$ cells.

To precise the phenotype and the frequency of $CD25^+FoxP3^+$Treg observed by

immunohistochemistry, flow cytometry analysis (**Fig.4A,B**) was performed on paired

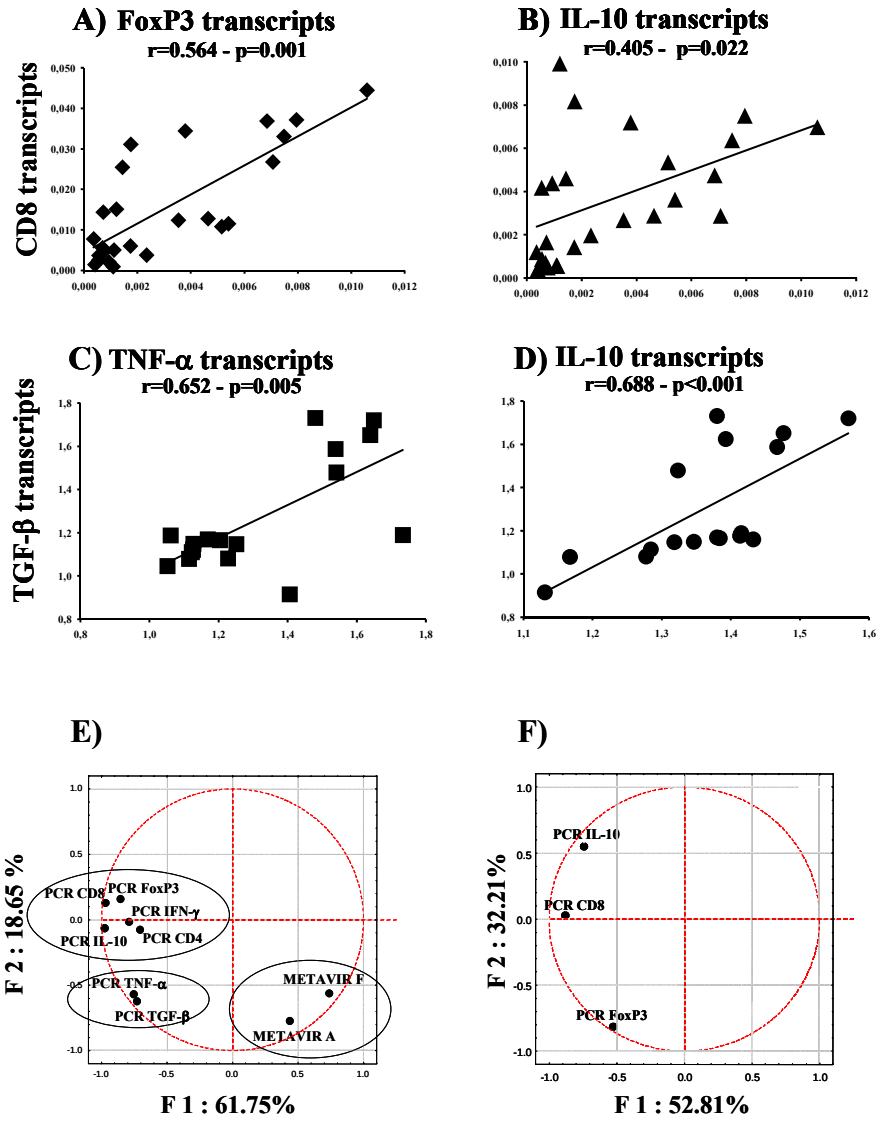

Fig.3. Relationship between expression levels of intra-hepatic immune markers.
(A,B) CD8 transcripts were significantly correlated with FoxP3 (**A**) and with IL-10 transcripts (**B**). **(C,D)** TGF-β transcripts were also strongly correlated with TNF-α (**C**) and with IL-10 transcripts (**D**). Principal Component Analysis (PCA) allowed defining gene expression clustering between CD8 and FoxP3 and IL-10 transcripts and between TGF-β and TNF-α and IL-10 transcripts. (**E,F**) PCA showed correlation circles of the most relevant clusters (**E**) and the correlation circle of the link between FoxP3, CD8 and IL-10 transcripts (**F**). Note that the first two factorial axes of the PCA analysis explain more than 80% of the total inertia.

fresh liver tissues and PBMC providing from the 8 additional CHC patients, whose characteristics did not differ from those of the 47 other CHC patients (**Table 1**). Among intra-hepatic $CD4^+$ lymphocytes, $CD4^+CD25^+$ and $CD4^+CD25^+FoxP3^+$ lymphocytes represented 6.0%±1.0% and 3.3%±1.5% respectively **(Fig.4C),** underlining that $CD4^+CD25^+FoxP3^+$ lymphocytes represented about 50% of $CD4^+CD25^+$ lymphocytes.Thus, intra-hepatic $CD4^+CD25^+FoxP3^+$ lymphocytes standed for less than 0.5% of the total intra-hepatic lymphocyte pool while no cell expressing $CD8^+$, $CD25^+$ and $FoxP3^+$ was detected in the liver. Frequencies for

peripheral lymphocyte subsets are shown in the **Table 3.**

Table 3. Quantification of intra-hepatic and peripheral lymphocytes in chronic HCV-infected patients (N=8)

Sub-populations of lymphocytes	intra-hepatic lymphocytes* (%)	peripheral lymphocytes* (%)
$CD4^+$ / total lymphocytes	16.6 ± 8.0	39.3 ± 13.6
$CD8^+$ / total lymphocytes	34.6 ± 5.9	26.7 ± 16.5
$CD4^+$ $CD25^+$ / $CD4^+$	6.0 ± 1.0	8.5 ± 5.4
$CD4^+$ $CD25^+FoxP3^+$ / $CD4^+CD25^+$	53.0± 20.0	43.5 ± 21.6
$CD4^+$ $CD25^+FoxP3^+$ / total lymphocytes	0.5 ± 0.1	1.5 ± 0.2
$CD8^+CD25^+FoxP3^+$ / $CD8^+CD25^+$	undetectable	0.1 ± 0.1

**Results were expressed in % (mean ± standard deviation)*

Notethat less than 0.1% of peripheral $CD8^+$ lymphocytes expressed $CD25^+FoxP3^+$.
Similar analysis achieved on 3 uninfected-HCV biopsies showed that frequency of $CD4^+CD25^+$ lymphocytes represented less than 0.1% of total lymphocytes and did not allow to detect $CD4^+CD25^+FoxP3^+$ lymphocytes (data not shown).

3.5. Relationship between immune markers and histological parameters.

We studied correlation between grade and stage of the disease according to the Metavir classification and intra-hepatic lymphocytes, quantitatively evaluated by immunohistochemical (n=20) and RT-PCR (n=47) analyses. Concerning Metavir necro-inflammatory grade, it was correlated with the total number of $CD4^+$ cells (r=0.526-p=0.017). The number of $CD8^+$ cells was higher along with Metavir activity grades, however this trend was not statistically significant (p=0.073). $FoxP3^+$ cells were two fold more abundant in livers with Metavir activity grade A1 than in those with Metavir grade A2, whereas their number was lower in livers with Metavir activity grade A3, but these differences were not statistically significant (**Fig.5A,B**). RT-PCR analyses showed that CD8 (r=0.547-p=0.001) and IL-10 (r=0.318-p=0.040) transcripts were the only parameters significantly correlated with Metavir activity grade. Concerning Metavir fibrosis stage, it was correlated with (i) total number of $CD4^+$ cells (r=0.713-p<0.001), (ii) total number of $CD8^+$ cells (r=0.714-p<0.001), (iii) number of $FoxP3^+$ cells in necro-inflammatory lesions (r=0.469-p=0.037), especially in piecemeal necrosis lesions (r=0.510-p=0.022). While the total number of $CD8^+$ cells was significantly higher along with Metavir fibrosis stages, the total number of $FoxP3^+$ cells was higher along with Metavir fibrosis stage F0 to stage F3 and was lower at the cirrhosis F4 stage in a non significantly way (**Fig.5C,D**). In addition, Metavir fibrosis stage was only correlated with CD8 (r=0.481-p=0.005) and

IL-10 (r=0.409-p=0.007) transcripts. Concerning the FoxP3^{+}/CD8^{+} cells ratio, it varied little from Metavir activity grade A1 to grade A3 and from Metavir fibrosis stage F0 to stage F3 **(Fig.5E,F).** Strikingly**,** it was significantly lower at the cirrhosis stage (Metavir fibrosis stage F3 to stage F4, median range: 3.5 vs 1.3 - z=2.324-p=0.024) **(Fig.5F).** Finally, it is worth to note that no correlation was found between serum viral load and any immune marker at cellular and transcriptional levels.

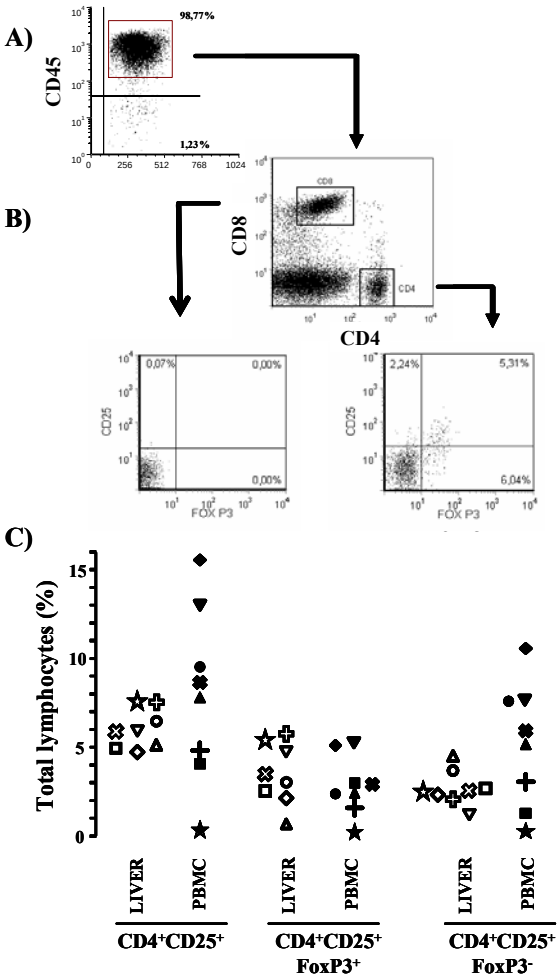

Fig.4. CD25/FoxP3 flow cytometry gating strategy. **(A)** Blood or intra-hepatic total lymphocytes were electronically separated on the basis of their CD45+ expression. **(B)** Total viable lymphocytes were gated on the basis of CD4^{+} or CD8^{+} expression. Then, each CD4^{+} or CD8^{+} population was gated on CD25 and FoxP3 expression**.** Finally, Treg were determined by evaluating CD25FoxP3 double positive cells. **(C)** Average percentages of each subpopulation CD4^{+}CD25^{+}, CD4^{+}CD25^{+}FoxP3^{+} and CD4^{+}CD25^{+}FoxP3^{-} were calculated for samples of patients from the liver (white symbols) and from the blood (black symbols).

4. Discussion

HCV-specific T-cell responses are generally weak, narrowly focused and often dysfunctional in CHC [8, 9]. The current debate is to determine whether Treg population plays a role in the immune dysfunction. To date, because of difficulty in obtaining HCV-infected liver tissue, Treg were mainly studied in PBMC samples, on cells expanded *in vitro* after HCV peptides stimulation [28]. We thus focused our analysis on intra-hepatic Treg, in direct *ex vivo* condition. Three complementary approaches were combined in order to characterize their phenotype, frequency and localization, to search for relationships with other immune markers and to assess their potential role in CHC pathogenesis.

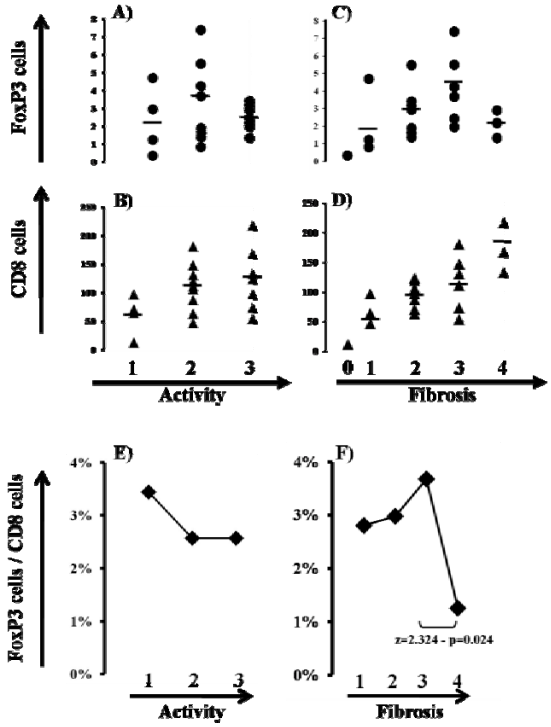

Fig.5. Relationship between the frequency of FoxP3 cells or CD8T lymphocytes and severity of disease according to Metavir scoring system.
(A-D) Number of FoxP3$^+$ cells and CD8$^+$T lymphocytes was presented according to Metavir activity grades **(A,B)** and Metavir fibrosis stages **(C,D). (E)** The ratio FoxP3/CD8 varied not significantly in patients with different Metavir activity grades. (**F**) Significant decrease of the ratio FoxP3/CD8 was observed in cirrhosis stage (F4)

The most important finding of our immunohistochemical study demonstrates that intra-hepatic Treg are mainly CD4$^+$FoxP3$^+$ cells while CD8$^+$FoxP3$^+$ cells are very scarce. This point is supported by our complementary flow cytometry analysis which does not detect CD8$^+$CD25$^+$FoxP3$^+$Treg in the liver samples. We confirm that CD8$^+$CD25$^+$FoxP3$^+$Treg are very low in blood as already published [27, 28, 33-35] and that the liver contains a population of CD4$^+$FoxP3$^+$ which does not express CD25, as reported in HCV [36] and HBV [37].

Another major immunohistochemical finding concerns the distribution of Treg in histological areas, showing that FoxP3$^+$ cells are predominantly localized in piecemeal and lobular necroses, in contact with CD8$^+$T cells. In addition, we confirm that CD4$^+$FoxP3$^+$ cells infiltrate the hepatic lymphoid aggregates, portal or septal tracts as well as parenchymatous lobules or nodules, in agreement with a previous study [38]. This would mean that Treg, within HCV-infected livers, have the direct access to interact with cytotoxic T cells at the site of action. Their plausible inhibitory role on the effector cells is supported by their localization together with CD8$^+$T cells, inside necro-inflammatory lesions. Furthermore, activated lymphocytes, either by viral or other antigens, which enter the liver are likely to encounter Treg since these cells are localized in portal tracts.

The next step was to determine if the presence of Treg and CD8T cells was related to cytokines. Our RT-PCR analysis reveals significant correlations between FoxP3 and CD8 transcripts and IL-10, TGF-β, TNF-α and IFN-γ. Moreover, PCA indicates gene expression clustering of CD8 with FoxP3 and IL-10 and of TGF-β with TNF-α and IL-10. The low number of immune cells in the liver does not allow assessing the kind of cells producing these cytokines. However, it is now established that IL-10 is mainly produced by T cells with regulatory or suppressive functions [39, 40]. Secretion of TGF-β, also produced by Treg, is considered as an important factor for the local survival and function of natural Treg [11, 41], but it also contributes to induction of fibrosis [42]. *In vitro* studies have demonstrated that both TGF-β and IL-10 inhibits the cytokine secretion and the cytotoxicity of CD8$^+$T lymphocytes [11, 43]. Considering our data and extrapolating the results achieved in PBMC, the correlation between the intra-hepatic cytokines TGF-β and IL-10 might favor synergistic effects on each other in (i) maintaining the Treg pool and (ii) reducing pro-inflammatory cytokine secretions. It is known that TNF-α production is induced and up-regulated in the liver by NS3 of HCV [44]. TNF-α intervenes at an early stage of

the cascade of events leading to liver damage [45] and is involved in the healing process including fibrogenesis [46]. As the majority (40/47) of patients included in our study have proven fibrosis, it was not surprising to detect high TNF-α expression in the liver of these patients. It has been also demonstrated that Treg inhibit *in vitro* production of IFN-γ by core specific $CD4^+$T cells and HCV-specific $CD8^+$T cells [13, 47]. As we found correlations between IL-10 and TGF-β, and between TNF-α and IFN-γ, one could speculate that the HCV inflammatory context favors production of both anti-inflammatory and pro-inflammatory cytokines. If Treg only partially inhibit the pool of intra-hepatic effector T cells, some effector cells could thus produce IFN-γ. These hypotheses are supported by previous data showing that IFN-γ is released by effector T cells in HCV infection [3, 5, 6]. Whatever the balance between the four cytokines, our regression analysis highlights strong correlations between FoxP3, CD8 and IL-10. This would mean that FoxP3, CD8 and IL-10 altogether establish a beneficial equilibrium for both the host and the virus. On one hand, the host would gain benefit from Treg which restrain $CD8^+$T lymphocytes, thus preventing liver damage. On the other hand, the virus would be preserved through the suppression of Treg on $CD8^+$T cells.

It is important to note that the number of $CD8^+$T cells is higher along with the necro-inflammatory activity and fibrosis, whereas the number of Treg is high up to Metavir activity grade A2 and Metavir fibrosis stage F3 but is low after this grade and stage. Interestingly, the $FoxP3^+/CD8^+$ cells ratio is significantly lower at the cirrhosis stage. In the light of these observations, the most likely scenario would be that, during the first steps of the disease, Treg modulate effector functions of T lymphocytes. During the cirrhosis end stage, when the tissue environment and the architecture are altered, Treg would be exhausted by the overflow of effector T cells. Interestingly, at different steps of the disease, no correlation was found between viral load and intra-hepatic Treg, suggesting that the essential role of Treg is to limit the $CD8^+$T cells pool. This would imply that the balance between Treg and effector lymphocytes is crucial to limit T lymphocytes-induced lesions. Therefore, the breakdown of equilibrium between FoxP3 and CD8T cells, up to stage F3, could appear to be a turning point in the course of the disease.

In conclusion, this study provides new insights in the phenotype of intra-hepatic Treg and their distribution in the different histological areas in chronic HCV-infected liver. It also suggests a link between Treg, CD8 and IL-10 which altogether could balance immune responses between the host and the virus, contributing to the viral persistence and preventing immunopathological liver tissue damages. It remains to determine whether the loss of Treg-CD8T cells interaction, beyond the stage F3, promotes an increase of cytolytic functions of CD8T lymphocytes, thus impacting on the expansion of liver damage.

Acknowledgements

We are grateful to the patients enrolled in this study for their cooperation. This work was supported by the institutional Grants from Institut National de la Santé et de la Recherche Médicale (INSERM), by a specific grant from the Agence Nationale pour la Recherche sur le Sida (ANRS), by specific support from Centre National de la Recherche Scientifique (CNRS), and in part by the "Biotherapic" and "AlphaVac" programs of the "Pôle de Compétitivité Lyon Biopôle". M.R. was supported by a fellowship from Higher Education Commission (HEC) of Pakistan; X.C. was supported by a fellowship from Région-Rhône Alpes actions in the "Clusters 10"; P.B. was supported by fellowships from French government and ANRS. We specifically thank Aurélie Dariz, Ingrid Esclozas and Alice Cheveau for their skilful assistance.

References

[1] Barnes E, Harcourt G, Brown D, Lucas M, Phillips R, Dusheiko G, et al. The dynamics of T-lymphocyte responses during combination therapy for chronic hepatitis C virus infection. Hepatology 2002;36:743-754.
[2] He XS, Rehermann B, Lopez-Labrador FX, Boisvert J, Cheung R, Mumm J, et al. Quantitative analysis of hepatitis C virus-specific CD8(+) T cells in peripheral blood and liver using peptide-MHC tetramers. Proc Natl Acad Sci U S A 1999;96:5692-5697.
[3] Wedemeyer H, He XS, Nascimbeni M, Davis AR, Greenberg HB, Hoofnagle JH, et al. Impaired effector function of hepatitis C virus-specific CD8+ T cells in chronic hepatitis C virus infection. J Immunol 2002;169:3447-3458.
[4] Grabowska AM, Lechner F, Klenerman P, Tighe PJ, Ryder S, Ball JK, et al. Direct ex vivo comparison of the breadth and specificity of the T cells in the liver and peripheral blood of patients with chronic HCV infection. Eur J Immunol 2001;31:2388-2394.
[5] Leroy V, Vigan I, Mosnier JF, Dufeu-Duchesne T, Pernollet M, Zarski JP, et al. Phenotypic and functional characterization of intrahepatic T lymphocytes during chronic hepatitis C. Hepatology 2003;38:829-841.
[6] Spangenberg HC, Viazov S, Kersting N, Neumann-Haefelin C, McKinney D, Roggendorf M, et al. Intrahepatic CD8+ T-cell failure during chronic hepatitis C virus infection. Hepatology 2005;42:828-837.
[7] Burton JR, Jr., Klarquist J, Im K, Smyk-Pearson S, Golden-Mason L, Castelblanco N, et al. Prospective analysis of effector and regulatory CD4+ T cells in chronic HCV patients undergoing combination antiviral therapy. J Hepatol 2008;49:329-338.
[8] Dustin LB, Rice CM. Flying under the radar: the immunobiology of hepatitis C. Annu Rev Immunol 2007;25:71-99.
[9] Thimme R, Oldach D, Chang KM, Steiger C, Ray SC, Chisari FV. Determinants of viral clearance and persistence during acute hepatitis C virus infection. J Exp Med 2001;194:1395-1406.
[10] Belkaid Y, Piccirillo CA, Mendez S, Shevach EM, Sacks DL. CD4+CD25+ regulatory T cells control Leishmania major persistence and immunity. Nature 2002;420:502-507.
[11] Cabrera R, Tu Z, Xu Y, Firpi RJ, Rosen HR, Liu C, et al. An immunomodulatory role for CD4(+)CD25(+) regulatory T lymphocytes in hepatitis C virus infection. Hepatology 2004;40:1062-1071.
[12] Hesse M, Piccirillo CA, Belkaid Y, Prufer J, Mentink-Kane M, Leusink M, et al. The pathogenesis of schistosomiasis is controlled by cooperating IL-10-producing innate effector and regulatory T cells. J Immunol 2004;172:3157-3166.
[13] MacDonald AJ, Duffy M, Brady MT, McKiernan S, Hall W, Hegarty J, et al. CD4 T helper type 1 and regulatory T cells induced against the same epitopes on the core protein in hepatitis C virus-infected persons. J Infect Dis 2002;185:720-727.
[14] McKee AS, Pearce EJ. CD25+CD4+ cells contribute to Th2 polarization during helminth infection by suppressing Th1 response development. J Immunol 2004;173:1224-1231.
[15] Sakaguchi S. Naturally arising CD4+ regulatory t cells for immunologic self-tolerance and negative control of immune responses. Annu Rev Immunol 2004;22:531-562.
[16] Claassen M, de Knegt R, Turgut D, Groothuismink A, Jansen H, Boonstra A. Role of multiple regulatory T cell populations in controlling peripheral blood and liver immunity to human hepatitis C virus infections. European Journal of Immunology 2009;39:S590.
[17] Shevach EM. CD4+ CD25+ suppressor T cells: more questions than answers. Nat Rev Immunol 2002;2:389-400.
[18] Sugimoto K, Ikeda F, Stadanlick J, Nunes FA, Alter HJ, Chang KM. Suppression of HCV-specific T cells without differential hierarchy demonstrated ex vivo in persistent HCV infection. Hepatology 2003;38:1437-1448.
[19] Dittmer U, He H, Messer RJ, Schimmer S, Olbrich AR, Ohlen C, et al. Functional impairment of CD8(+) T cells by regulatory T cells during persistent retroviral infection. Immunity 2004;20:293-303.
[20] Rushbrook SM, Ward SM, Unitt E, Vowler SL, Lucas M, Klenerman P, et al. Regulatory T cells suppress in vitro proliferation of virus-specific CD8+ T cells during persistent hepatitis C virus infection. J Virol 2005;79:7852-7859.
[21] Kim JM, Rudensky A. The role of the transcription factor Foxp3 in the development of regulatory T cells. Immunol Rev 2006;212:86-98.
[22] Ziegler SF. FOXP3: of mice and men. Annu Rev Immunol 2006;24:209-226.
[23] Ebinuma H, Nakamoto N, Li Y, Price DA, Gostick E, Levine BL, et al. Identification and in vitro expansion of functional antigen-specific CD25+ FoxP3+ regulatory T cells in hepatitis C virus infection. J Virol 2008;82:5043-5053.
[24] Li S, Gowans EJ, Chougnet C, Plebanski M, Dittmer U. Natural regulatory T cells and persistent viral infection. J Virol 2008;82:21-30.
[25] Accapezzato D, Francavilla V, Paroli M, Casciaro M, Chircu LV, Cividini A, et al. Hepatic expansion of a virus-specific regulatory CD8(+) T cell population in chronic hepatitis C virus infection. J Clin Invest 2004;113:963-972.
[26] Bienvenu B, Martin B, Auffray C, Cordier C, Becourt C, Lucas B. Peripheral CD8+CD25+ T

lymphocytes from MHC class II-deficient mice exhibit regulatory activity. J Immunol 2005;175:246-253.
[27] Shevach EM. From vanilla to 28 flavors: multiple varieties of T regulatory cells. Immunity 2006;25:195-201.
[28] Billerbeck E, Blum HE, Thimme R. Parallel expansion of human virus-specific FoxP3- effector memory and de novo-generated FoxP3+ regulatory CD8+ T cells upon antigen recognition in vitro. J Immunol 2007;179:1039-1048.
[29] Bonorino P, Ramzan M, Camous X, Dufeu-Duchesne T, Thelu MA, Sturm N, et al. Fine characterization of intrahepatic NK cells expressing natural killer receptors in chronic hepatitis B and C. J Hepatol 2009;51:458-467.
[30] Bonorino P, Leroy V, Dufeu-Duchesne T, Tongiani-Dashan S, Sturm N, Pernollet M, et al. Features and distribution of CD8 T cells with human leukocyte antigen class I-specific receptor expression in chronic hepatitis C. Hepatology 2007;46:1375-1386.
[31] Pernollet M, Jouvin-Marche E, Leroy V, Vigan I, Zarski JP, Marche PN. Simultaneous evaluation of lymphocyte subpopulations in the liver and in peripheral blood mononuclear cells of HCV-infected patients: relationship with histological lesions. Clin Exp Immunol 2002;130:518-525.
[32] Vigan I, Jouvin-Marche E, Leroy V, Pernollet M, Tongiani-Dashan S, Borel E, et al. T lymphocytes infiltrating the liver during chronic hepatitis C infection express a broad range of T-cell receptor beta chain diversity. J Hepatol 2003;38:651-659.
[33] Bisikirska B, Colgan J, Luban J, Bluestone JA, Herold KC. TCR stimulation with modified anti-CD3 mAb expands CD8+ T cell population and induces CD8+CD25+ Tregs. J Clin Invest 2005;115:2904-2913.
[34] Endharti AT, Rifa IMs, Shi Z, Fukuoka Y, Nakahara Y, Kawamoto Y, et al. Cutting edge: CD8+CD122+ regulatory T cells produce IL-10 to suppress IFN-gamma production and proliferation of CD8+ T cells. J Immunol 2005;175:7093-7097.
[35] Noble A, Giorgini A, Leggat JA. Cytokine-induced IL-10-secreting CD8 T cells represent a phenotypically distinct suppressor T-cell lineage. Blood 2006;107:4475-4483.
[36] Franceschini D, Paroli M, Francavilla V, Videtta M, Morrone S, Labbadia G, et al. PD-L1 negatively regulates CD4+CD25+Foxp3+ Tregs by limiting STAT-5 phosphorylation in patients chronically infected with HCV. J Clin Invest 2009;119:551-564.
[37] Stoop JN, Claassen MA, Woltman AM, Binda RS, Kuipers EJ, Janssen HL, et al. Intrahepatic regulatory T cells are phenotypically distinct from their peripheral counterparts in chronic HBV patients. Clin Immunol 2008;129:419-427.
[38] Ward SM, Fox BC, Brown PJ, Worthington J, Fox SB, Chapman RW, et al. Quantification and localisation of FOXP3+ T lymphocytes and relation to hepatic inflammation during chronic HCV infection. J Hepatol 2007;47:316-324.
[39] Abel M, Sene D, Pol S, Bourliere M, Poynard T, Charlotte F, et al. Intrahepatic virus-specific IL-10-producing CD8 T cells prevent liver damage during chronic hepatitis C virus infection. Hepatology 2006;44:1607-1616.
[40] Billerbeck E, Thimme R. CD8+ regulatory T cells in persistent human viral infections. Hum Immunol 2008;69:771-775.
[41] Bolacchi F, Sinistro A, Ciaprini C, Demin F, Capozzi M, Carducci FC, et al. Increased hepatitis C virus (HCV)-specific CD4+CD25+ regulatory T lymphocytes and reduced HCV-specific CD4+ T cell response in HCV-infected patients with normal versus abnormal alanine aminotransferase levels. Clin Exp Immunol 2006;144:188-196.
[42] Schuppan D, Krebs A, Bauer M, Hahn EG. Hepatitis C and liver fibrosis. Cell Death Differ 2003;10 Suppl 1:S59-67.
[43] Uraushihara K, Kanai T, Ko K, Totsuka T, Makita S, Iiyama R, et al. Regulation of murine inflammatory bowel disease by CD25+ and CD25-CD4+ glucocorticoid-induced TNF receptor family-related gene+ regulatory T cells. J Immunol 2003;171:708-716.
[44] Hassan M, Selimovic D, Ghozlan H, Abdel-Kader O. Induction of high-molecular-weight (HMW) tumor necrosis factor(TNF) alpha by hepatitis C virus (HCV) non-structural protein 3 (NS3) in liver cells is AP-1 and NF-kappaB-dependent activation. Cell Signal 2007;19:301-311.
[45] McGuinness PH, Painter D, Davies S, McCaughan GW. Increases in intrahepatic CD68 positive cells, MAC387 positive cells, and proinflammatory cytokines (particularly interleukin 18) in chronic hepatitis C infection. Gut 2000;46:260-269.
[46] Migita K, Abiru S, Maeda Y, Daikoku M, Ohata K, Nakamura M, et al. Serum levels of interleukin-6 and its soluble receptors in patients with hepatitis C virus infection. Hum Immunol 2006;67:27-32.
[47] Boettler T, Spangenberg HC, Neumann-Haefelin C, Panther E, Urbani S, Ferrari C, et al. T cells with a CD4+CD25+ regulatory phenotype suppress in vitro proliferation of virus-specific CD8+ T cells during chronic hepatitis C virus infection. J Virol 2005;79:7860-7867.